AD-A036 481 HUGHES RESEARCH LABS MALIBU CALIF F/G 17/2
THIN FILM OPTICAL SWITCH.(U)
FEB 77 B U CHEN, G L TANGONAN N00173-76-C-0113
NL

UNCLASSIFIED

| OF |
AD
A036481

END

DATE
FILMED
3-77

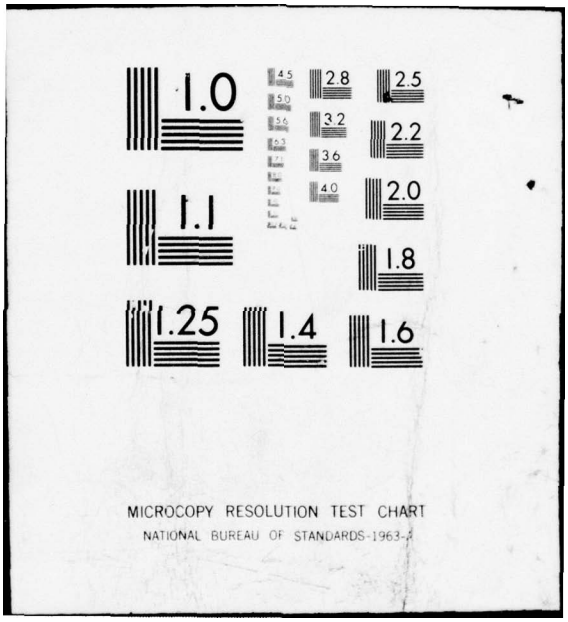
1.0
1.1
1.25
1.4
1.6
1.8
2.0
2.2
2.5
2.8
3.2
3.6
4.0
4.5
5.0
5.6
6.3
MICROCOPY RESOLUTION TEST CHART
NATIONAL BUREAU OF STANDARDS-1963-A

AD A036481

12

06

THIN FILM OPTICAL SWITCH

Bor Chen and Gregory Tangonan

Hughes Research Laboratories
3011 Malibu Canyon Road
Malibu, CA 90265

DDC
DISTRIBUTED
MAR 7 1977
C

February 1977

Contract N00173–76–C–0113
Final Report
For Period 22 October 1976 through 21 January 1977

Approved for public release; distribution unlimited.

Sponsored By
NAVAL RESEARCH LABORATORY
4555 Overlook Avenue, S.W.
Washington, DC 20375

UNCLASSIFIED

SECURITY CLASSIFICATION OF THIS PAGE (When Data Entered)

REPORT DOCUMENTATION PAGE	READ INSTRUCTIONS BEFORE COMPLETING FORM
1. REPORT NUMBER	2. GOVT ACCESSION NO. 3. RECIPIENT'S CATALOG NUMBER
4. TITLE (and Subtitle) THIN FILM OPTICAL SWITCH.	5. TYPE OF REPORT & PERIOD COVERED Final report, 22 Oct 1976- 21 Jan 1977
	6. PERFORMING ORG. REPORT NUMBER
7. AUTHOR(s) Bor Chen and Gregory Tangonan	8. CONTRACT OR GRANT NUMBER(s) N00173-76-C-0113
9. PERFORMING ORGANIZATION NAME AND ADDRESS Hughes Research Laboratories 3011 Malibu Canyon Road Malibu, CA 90265	10. PROGRAM ELEMENT, PROJECT, TASK AREA & WORK UNIT NUMBERS
11. CONTROLLING OFFICE NAME AND ADDRESS Naval Research Laboratory 4555 Overlook Ave., S.W. Washington, D.C. 20375	12. REPORT DATE February 1977 13. NUMBER OF PAGES 31 p.
14. MONITORING AGENCY NAME & ADDRESS (if different from Controlling Office)	15. SECURITY CLASS. (of this report) Unclassified 15a. DECLASSIFICATION/DOWNGRADING SCHEDULE

16. DISTRIBUTION STATEMENT (of this Report)

Approved for public release; distribution unlimited.

DDC RECEIVED MAR 7 1977 C

17. DISTRIBUTION STATEMENT (of the abstract entered in Block 20, if different from Report)

18. SUPPLEMENTARY NOTES

19. KEY WORDS (Continue on reverse side if necessary and identify by block number)

Integrated optics, Optical channel waveguide, Optical switch, Taper coupler

20. ABSTRACT (Continue on reverse side if necessary and identify by block number)

This report, together with three previous quarterly reports, presents the design, development, fabrication and evaluation of a wideband optical switch based on the deflection of two dimensionally confined beams by electro-optically controlled phase grating. The waveguide medium is Ti-diffused $LiNbO_3$. An interdigital electrode is placed on the overlapped region of two crossed channel waveguides. When a voltage is applied to the electrode, a Bragg phase grating is formed so that the

over

DD FORM 1 JAN 73 1473 EDITION OF 1 NOV 65 IS OBSOLETE

UNCLASSIFIED

SECURITY CLASSIFICATION OF THIS PAGE (When Data Entered)

AB

172600

micrometers

optical beam in one channel waveguide is deflected into the opposite one. In order to interface the switching device to single mode optical fibers, 4 μm wide single mode channel waveguides are employed at the input and output ports. These waveguides are expanded adiabatically through slowly tapered sections into wide multimode channel waveguides (30 μm) that intersect in the grating interaction region.

The design of efficient expansion and contraction tapers was a crucial part of this program. As a first cut at the problem, linear tapers of taper lengths 300, 600, 900 and 1200 μm were designed to expand channel guides from a 4 μm single mode channel to a 70 μm multimode channel. However, the measurement of coupling efficiency for TE and TM polarizations indicated that linear tapers were not efficient to preserve the mode structure even when the taper length is 1200 μm, 4000 times the He-Ne laser wavelength in the waveguide. A modification of initial switch design was incorporated into the program. In the new switch design, the width of expanded channel section was reduced from 70 μm to 30 μm and a taper formed out of three linear segments was adopted. The channel waveguide width is expanded from 4 μm to 10 μm by the first linear taper of length 500 μm and from 20 μm to 30 μm by the third linear taper of length 800 μm. The full angles of these tapers are 1.72°, 1.15°, and 0.72°, respectively. The experimental result indicated that the program goal of single mode coupling efficiency of 90% per taper for TM polarization had been achieved.

The second experimental phase involved the development of Bragg grating and integration with crossed channel waveguides. The grating is an interdigital electrode of spacing 4 μm and length 0.5 mm. TE polarization light (He-Ne laser) was coupled into one channel guide at the input port. The power coming out of the channel guides at the output port was monitored as the voltage applied to the electrode varied. For sample NB 23, maximum switching efficiency (20%) occurred at 12.5 volts. Although the switching efficiency was lower than what we expected, we believe all the lowest order mode was deflected as evidenced by the fact the switching efficiency obeyed the $\sin^2$ BV voltage dependence function and reached the maximum value at 12.5 volts. Most of the power remained in the undeflected channel guides were Li out-diffused modes generated at expansion taper section and at Bragg grating region. We have developed a technique (under separate IRD funding) to eliminate Li out-diffusion waveguide by annealing the samples in $LiNbO_3$ powder. The interaction between metal electrode and optical beam can be avoided with a thin buffer layer (for instance, 2000 Å SiO_2) evaporated on the waveguide. With these improvements incorporated into the device, switching efficiency greater than 80% can be expected.

The drive power per bandwidth of optical switch is given by $\frac{\pi}{2} C V_m^2$, where C is the electrode capacitance and V_m is the applied voltage for maximum switching efficiency. For the switch we fabricated, V_m = 12.5 volts and C = 2.2 pF, the drive power per bandwidth is 0.16 mW/MHz. If the device is operated at bandwidth of 3 GHz, the drive power required is about 5 W.

TABLE OF CONTENTS

LIST OF ILLUSTRATIONS

PREFACE

The following personnel contributed to the research work reported here: B. U. Chen, G. L. Tangonan, and A. Lee. The photomasks were fabricated by the photolithography services of Hughes Aircraft Company, Fullerton, California, under the direction of W. Gray and G. Bair.

I. Introduction

The field of optical communications, which began with the successful development of low loss optical fiber waveguides in early 1970's, has been emerging as a new technology which promises significant cost and performance advantages over conventional communication systems. The use of optical transmission circuits greatly reduces size and weight requirements, increases high bandwidth capability, eliminates electromagnetic interference, and provides a high degree of intercept security and dielectric isolation. An area of optical communications attracting much research activity is the switching of optical beams. This program addresses an approach that leads to the development of a wideband switching capability for handling optical signals in a communication network. The program goal involves the design and fabrication of an optical switch based on the deflection of two dimensionally confined beams by electro-optically controlled phase grating.

The switch is of double-pole-double-throw (DPDT) type. The waveguide medium is Ti-diffused $LiNbO_3$. $LiNbO_3$ has excellent electro-optic properties and the waveguides thus formed have very good optical quality (waveguide loss $\lesssim$ 1 dB/cm). Figure 1 is an illustration of the switching format. An interdigital electrode is placed on the overlapped region of two crossed channel waveguides. When a voltage is applied to this electrode, it forms a Bragg phase grating through electro-optic interactions. The crossed angle and grating spacing are designed so that the first order Bragg reflection condition is satisfied. As a result, the optical beam in one channel waveguide is deflected into the opposite one. In order to interface the switching device to single mode optical fibers, narrow (4 μm wide) single mode channel waveguides are used at both input and output ports. These waveguides are expanded adiabatically through slowly tapered sections into wide, multimode channel waveguides (30 μm) that intersect in the grating interaction region. The Bragg grating spacing is 4 μm and the channel guides crossed angle is 4°6'. One important feature of this approach is that all the components of switch can be fabricated using well developed photolithographic technique.

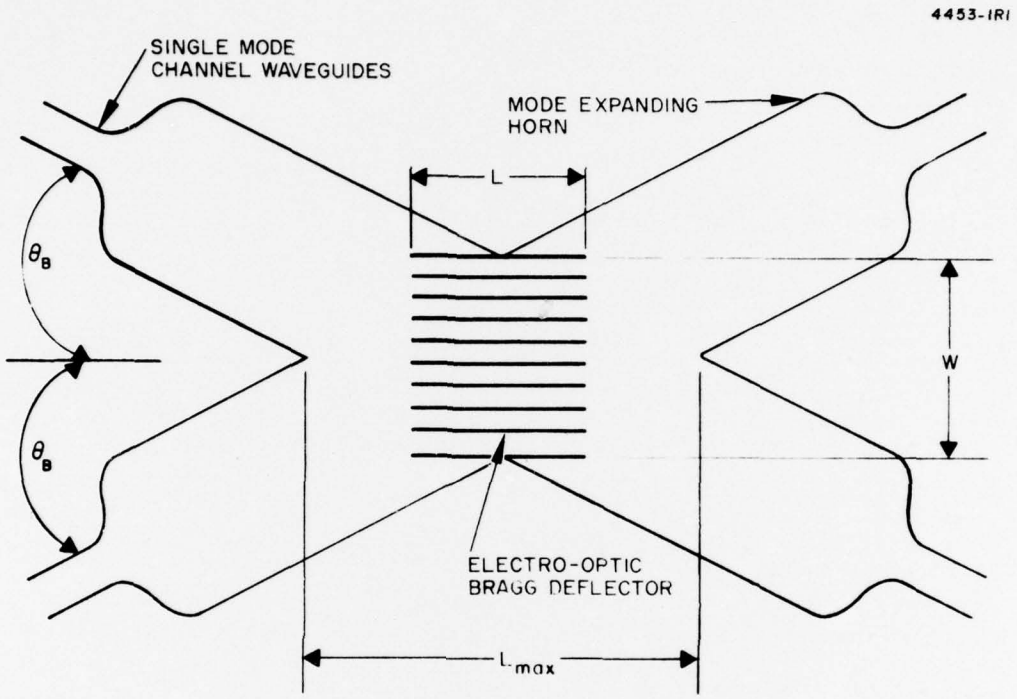

Fig. 1. Optical switch using electro-optic Bragg deflectors

The design of expansion and contraction tapers is the crucial part of this program. If the taper is sufficiently gentle, the lowest order mode will be transmitted adiabatically, continuously readjusting to the slow variation of the guide width with virtually no reflection or coupling to higher order modes. In reality, one has to sacrifice the perfect adiabatic coupling in order to use a taper of reasonable length. During the development stage of this program, a curved taper of three linear segments with total length of 1.5 mm is designed. The goal of 90% single mode transmission efficiency (per taper) is achieved for such tapers connecting channel waveguides of width 4 μm and 30 μm.

Optical waveguide modulators/switches have several advantages over their bulk counterparts. In channel waveguide devices, the optical beams are confined to travel essentially unlimited interaction length. In addition, the channel waveguides usually have cross-sectional dimensions on the order of optical wavelength. Strong electro-optic interaction between guided optical beam and fringe field of surface electrode can occur at much lower applied voltage. As a result, a numerous saving in specific energy (the drive power required per unit bandwidth to obtain a modulation depth equivalent to an intensity modulation depth of 84%) can be expected. It is estimated that for λ = 1 μm and interaction L = 1 mm, the specific energy can be reduced by more than three orders of magnitude when compared to bulk devices. We estimated that the drive power as low as 5.0 W can be realized for 3 GHz bandwidth performance.

II. Summary of Previous Report

Much of the work on this program has been reported in the three quarterly technical reports already submitted.[1,2,3] We include here outlines of the contents of these three reports.

A. Channel Waveguide Fabrication

Waveguides of straight and tapered channels were fabricated by diffusing e-beam evaporated Ti into y-cut $LiNbO_3$ substrates. The diffusion pattern of Ti metal was cut by the lift-off photolithographic technique. Ti metal was evaporated onto the photoresist pattern

subsequent to exposure and development of the photoresist. The open area of the resist was thus filled with Ti metal while unwanted Ti on the photoresist was removed by dissolving the resist (Shipley AZ 1350B) in acetone. Diffusions were normally carried out in the temperature range from 850°C to 950°C in a flowing oxygen atmosphere. The diffusion time varied from 5 to 16 hours. Before diffusion, Ti-metal had been oxidized to TiO_2 at a relatively lower temperature (for instance, 600°C). Single mode channel waveguides were formed by diffusing 4 μm wide 200 Å thick Ti stripe into $LiNbO_3$ substrates. The waveguide loss of planar waveguides thus formed was measured to be about 1 dB/cm. While the loss measurement became difficult for 4 μm wide single mode channel guide, we estimated the loss figure was in the same rank as planar waveguides.

After diffusion, the channel waveguides formed ridges of height about 2.5-3.0 times the original Ti-thickness. Further studies indicated that the ridge height was increased by nearly the same factor right after the oxidation stage when TiO_2 was formed. The ridge formation, as a registration mark, facilitates the alignment of Bragg electrode to the channel waveguide in latter processing.

B. *Lateral Spread of Channel Waveguide*

The coupling efficiency of a given taper structure depends strongly on the expansion ratio (final width to initial channel width). So it is important to know the amount of lateral diffusion which determines the final diffused channel width. We have studied the Ti concentration profile near the edge of a strip of 70 μm initial width using electron microprobe technique. No enhanced lateral diffusion was observed.

Figure 2 shows the result of electron microprobe measurements of a channel guide in sample 5. The solid curve in Fig. 2 is a complementary error function with the parameter of diffusion depth $2\sqrt{D_z t}$ adjusted to give the best fit. The diffusion constant of Ti in C-axis is then given by

$$2\sqrt{D_z t} = 12.86\ \mu m$$
$$D_z = 2 \times 10^{-8}\ cm^2/hour$$

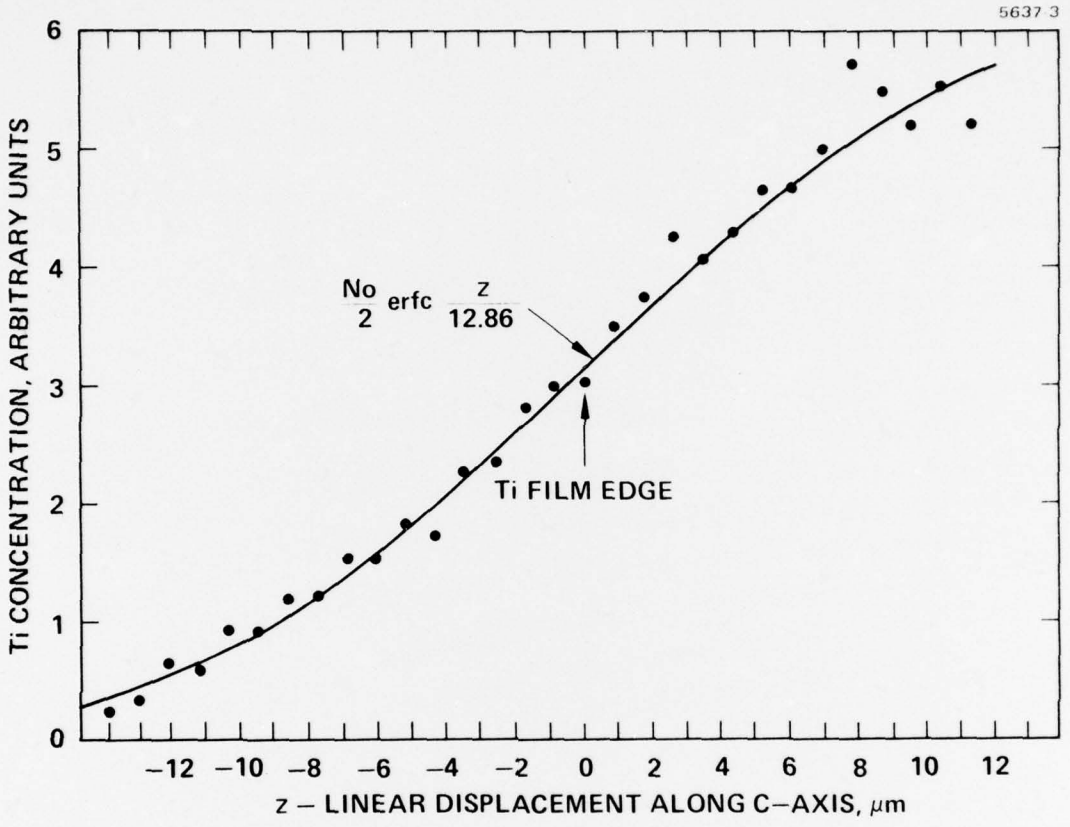

Fig. 2. Distribution of Ti near the edge of a stripe of 70 μm initial width.

The Ti concentration was down by another factor of 2 at position about 6 μm from the edge. Compared to this number with the downward diffusion depth of about 4 μm, we concluded that enhanced lateral diffusion is not observed in this study.

C. Linear Taper Coupling Efficiency Measurement

As the first cut to the expansion and contraction taper structures, linear tapers of taper lengths of 300, 600, 900 and 1200 μm were designed to expand channel guides from a 4 μm single mode channel to a 70 μm multimode channel. These taper lengths correspond roughly to 1000, 2000, 3000 and 4000 λ where λ is the He-Ne laser wavelength in the guide. The linear taper waveguide structure under test consists of a 4 μm single mode channel guide section, a linear expansion taper section, a 70 μm multimode channel guide section, a linear contraction taper section, and 4 μm single mode channel guide section. We measured the single mode transmission efficiency between two 4 μm wide single mode channel guide sections. By comparing the output power of the taper structure with that of the neighboring 4 μm straight channel guide, the throughput of the structure of one expansion taper and one contraction taper was determined. Assuming the expansion taper and contraction taper have the same coupling efficiency, we define the square root of the throughput as the taper coupling efficiency.

Figure 3 shows the averaged value of coupling efficiency for both TE and TM waves as a function of the taper length. As shown in the figure, the coupling efficiency for TM wave was much lower than for TE wave. The reason is the following. Lithium and oxygen escaped out of the $LiNbO_3$ substrate when the Ti in-diffusion process was performed at high temperature. The out-diffusion process resulted in an increase in the extraordinary index of refraction. As a result, in addition to the Ti in-diffused channel waveguides, there is an additional planar Li_2O out-diffusion waveguide for TE polarization wave when the light propagates in the x-axis. In the TE wave measurement, those out-diffusion modes were coupled out together with the in-diffusion guided mode, hence, a wrong reading of higher output power was obtained. Because the throughput of linear tapers obtained in the experiment is not as high as the 90% required throughput for the optical switch design, a modification of initial switch design was made and incorporated into the final devices.

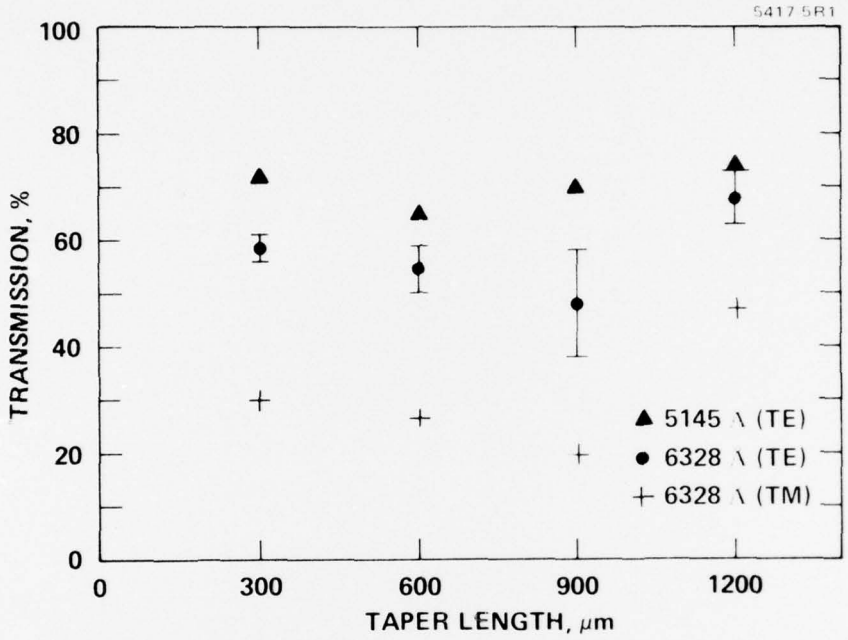

Fig. 3. Single mode coupling efficiency of linear tapers as a function of the taper length.

D. Modification of Initial Switch Design

In order to achieve the goal of 90% single mode transmission efficiency, the width of expanded channel section was reduced from 70 μm to 30 μm and a taper formed out of three linear segments was adopted. Figure 4 shows the new photomask design for single taper waveguide as well as crossed taper waveguide. The four legs of crossed taper waveguides are bent to parallel to the straight channel guides at a distance of 8 mm from the center of overlapped area. Figure 5 shows the three linear sections of coupling horn structure. The channel waveguide width is expanded from 4 μm to 10 μm by the first linear taper of length 200 μm, from 10 μm to 20 μm by the second linear taper of length 500 μm and from 20 μm to 30 μm by the third linear taper of length 800 μm. The full angles of these tapers are 1.72°, 1.15°, and 0.72°, respectively. The total length of this coupling horn structure is 1.5 mm.

To ensure that Bragg scattering into a well defined direction occurs with optimum efficiency, there must be sufficient number of grating lines that intersected by the beam incident at the Bragg angle, θ_B. As the width of expanded channel section is reduced from 70 μm to 30 μm, the grating design is also changed by reducing the spacing from the original 7 μm to 4 μm. This 4 μm spacing grating is readily achieved by conventional photolithography. In this way, 7.5 periods of interdigital electrodes can be accommodated in the waveguide overlapped area. Because the grating period is smaller, the necessary grating length can also be cut down to 0.5 mm without affecting the value of Q parameter which governs the deflection process. Table 1 lists all the important parameters for new switch designs. The dimensions of Bragg electrode structure are shown in Fig. 6.

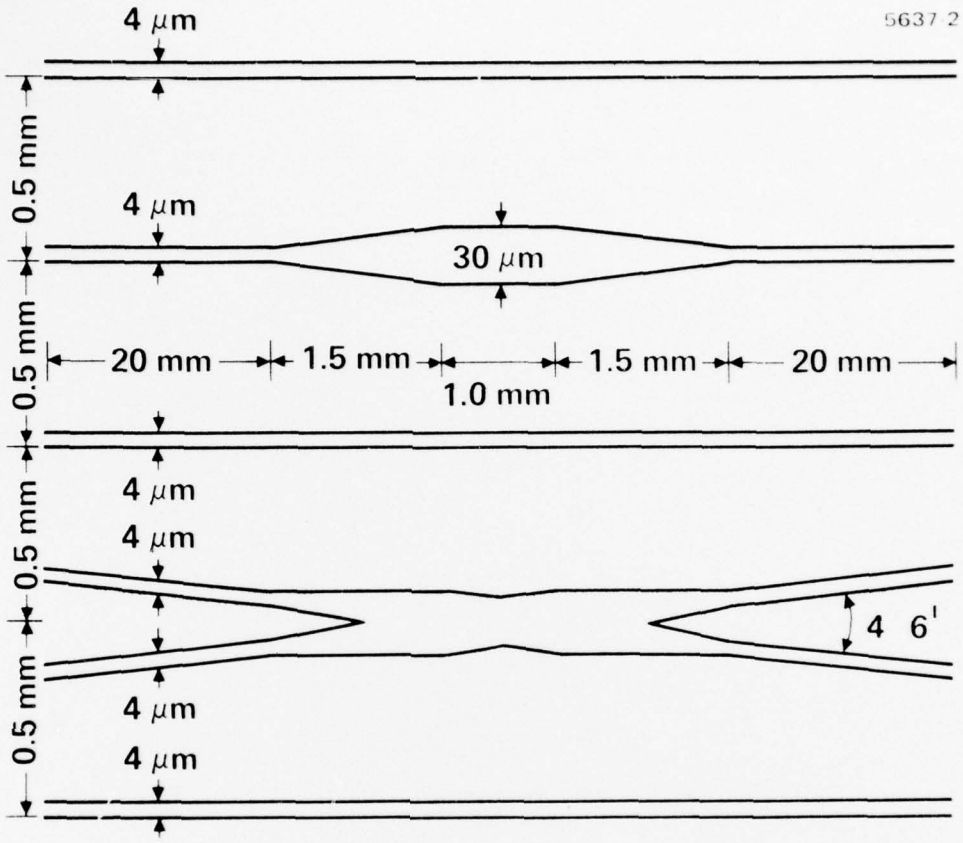

Fig. 4. Photomask design for curved taper waveguides.

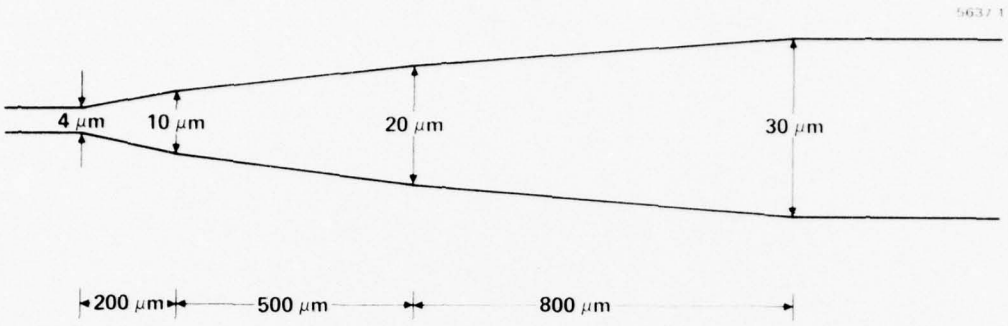

Fig. 5. Three linear sections for coupling horn structure.

Table 1

Bragg Switch Design Parameters

Width of Expended Channel Section, W.	30 μm
Total Length of Curved Taper	1.5 mm
Bragg Angle, θ_B	2°3'
Periodicity, Λ	4.0 μm
Number of Periods, N	10
Bragg electrode length, L	0.5 mm
Q parameter, $Q = \frac{2\pi\lambda_o L}{n \Lambda^2}$	19 π
Total Length of Switch Device (including coupling tapers)	4.0 mm

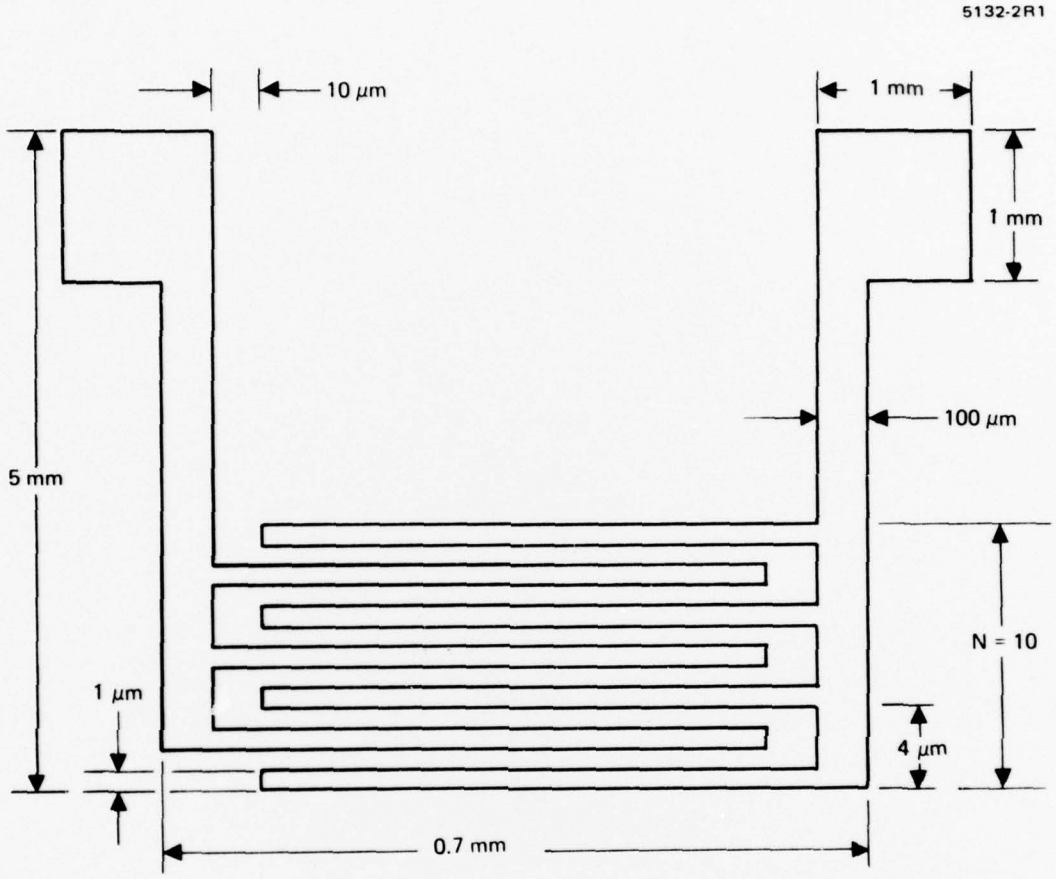

Fig. 6. Dimensions of Bragg electrode

E. Curved Taper Coupling Efficiency Measurement

Waveguide structures with the shaped taper design have been fabricated on $LiNbO_3$ substrates. The experimental result indicates that a single mode to single mode coupling efficiency of 90% per taper for TM polarization has been achieved. The crosstalk between two intersecting channel guides as a result of the absence of lateral confinement over a portion of the region of intersection was considered as a potential problem. However, no crosstalk was observed to the naked eye when viewing the output modes of crossed tapers.

III. Switch Device Fabrication and Evaluation

A. Electrode Fabrication

During the fourth quarter of this program, effort was concentrated on the fabrication of Bragg interdigital electrode. The electrode has spacing 4 μm with electrode gap to width ratio 1.0. The resolution of 1 μm wide lines of the electrode structure is the state-of-the-art of conventional photolithography. Special measures had been taken to assure a good contact between the photomask and $LiNbO_3$ channel waveguides. K&D Photomask Aligner with modified sample holder was used to align the photomask to the crossed channel guide. The details of the photolithographic processing are listed in Table II. After many trials of different parameters of resist, we were able to fabricate almost perfect electrode pattern. Once the photoresist pattern was formed, the sample was put in the vacuum system and coated with about 1500 Å thick aluminum. Lift-off technique was used again to remove unwanted Al by dissolving photoresist in acetone ultrasonically. Figure 7(a) shows the alignment of the final metal electrode to the crossed channel waveguide. Figure 7(b) is the photograph of detailed electrode structure. The dots in the picture are dust particles and scratches in the microscope.

5916-1

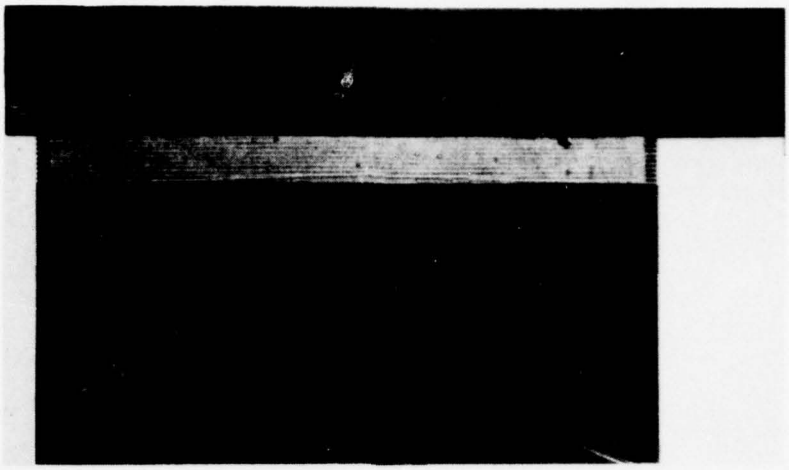

Fig. 7(a) Arrangement of electrodes and crossed channel waveguide

5916-2

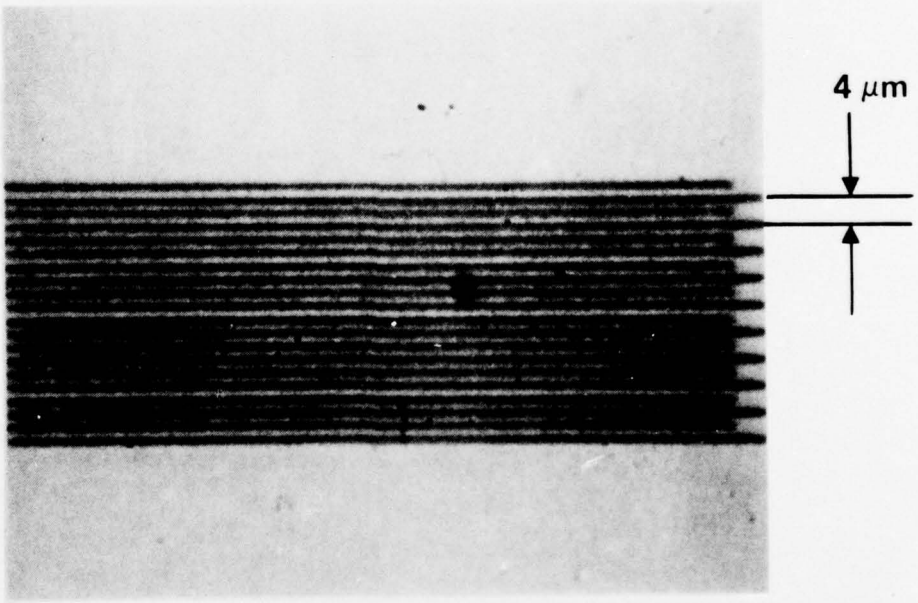

Fig. 7(b) High magnification of 4 μm spacing electrode structure

Fig. 7 (a) Arrangement of electrode and crossed channel waveguide (b) high magnification of 4 μm spacing electrode structure.

Table II

Fabrication of Electrode on Photoresist

Photoresist	Shipley AZ 1350B filtered through 0.5 μm membrane
Coating	3500 RPM
Prebaking	80°C, 20 to 30 min
Exposure	25 sec
Developing solution	Shipley AZ Developer: DI water 1:1
Developing time	30 sec
Rinse	DI water 2 min

B. Bragg Deflection Measurement

The evaluation of Bragg switch performance was carried out using two coupling prisms. Figure 8 describes the experimental arrangement. Two rutile (TiO_2) prisms were placed on a 4 μm wide single mode channel guide section. TE polarization He-Ne laser light (λ_o = 6328 Å) was coupled into the top channel on the left. With zero applied voltage, the guided beam was undeflected and coupled out from the bottom channel on the right. Upon application of a switching voltage to the interdigital electrodes, the beam was deflected upward by 2 θ_B into the opposite channel waveguide. The switching device is designed for Bragg deflection of the lowest order mode.

Higher order modes are present at interaction region as the result of finite expansion taper length as well as the scattering of the metal electrode. These are also involved in Bragg deflection as the lowest order mode because of the uncertainty of the grating momentum, $\Delta k_{gr} = \frac{2\pi}{N\Lambda}$. However, the deflected higher order modes radiate before they reach the 4 μm single mode channel section at output port. The power coupled out of the top channel on the right was measured as a function of applied voltage.

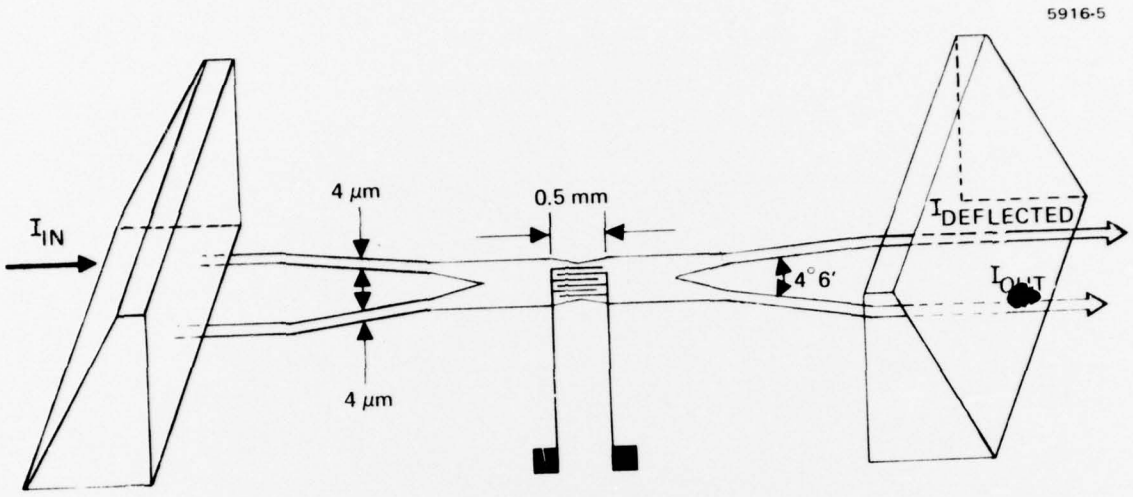

Fig. 8. Experimental arrangement of switching efficiency measurement

Two devices, NB 21 and NB 23, were fabricated and tested. They were diffused at 950°C for 5 hours. On each sample, there are two Bragg switch devices, one in the center and one near the edge. Figures 9 and 10 show the normalized deflection efficiency versus applied voltage for the central switch on each sample. Electrode on NB 21 had several breaks in the lines. The peak deflection ($\sim$18%) occurred at V = 33.5 volts. The electrical breakdown occurred as the applied voltage was raised up to 50 volts. The electrode structure on NB 23 was excellent. This was verified by the fact that maximum deflection ($\sim$20%) occurred at applied voltage as low as 12.5 volts. The solid lines in Figs. 9 and 10 are theoretical curves of $\sin^2 BV$ normalized at maximum deflected efficiency. B is a constant depending on overlap integral of electrical and optical fields. As indicated in the figure, the behavior of the experimental points is in good agreement with theoretical prediction.

C. Measures of Merit

(a) Crosstalk

The basic function of an optical switch is to move the guided beam from one channel to another. One of the most important measures of merit is the isolation between two channel guides. In this experiment, the nature of the crosstalk problem is two-fold. First, crosstalk may occur purely as a result of the intersection of the two guide channels. Within the region of intersection the beams propagate with no lateral confinement over a portion of this region and with only partial lateral confinement over the remaining portion. Thus leakage may occur from one channel to the other due to diffraction in this region. Second, crosstalk may occur due to the presence of the interdigital electrodes, in the "off" as well as the "on" state, as a result of scattering into the wrong channel or of incomplete diffraction into the desired channel. As we mentioned in the third quarterly report, there is essentially no crosstalk (< 30 dB) between the two channel guides before the metallic electrode was incorporated into the waveguides. With the presence of metallic grating structure, a crosstalk of -20 dB was measured. This number can be reduced substantially by forming a thin electric buffer layer (for instance 2000 Å SiO_2) to isolate the guided optical beam from the metallic electrode.

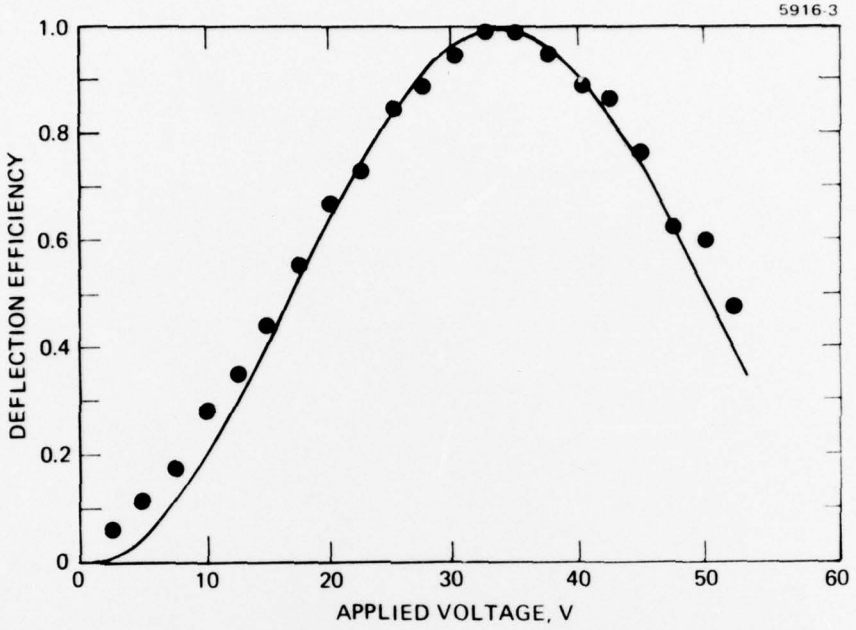

Fig. 9 Deflection efficiency vs. applied voltage for e-o Bragg switch (NB 21)

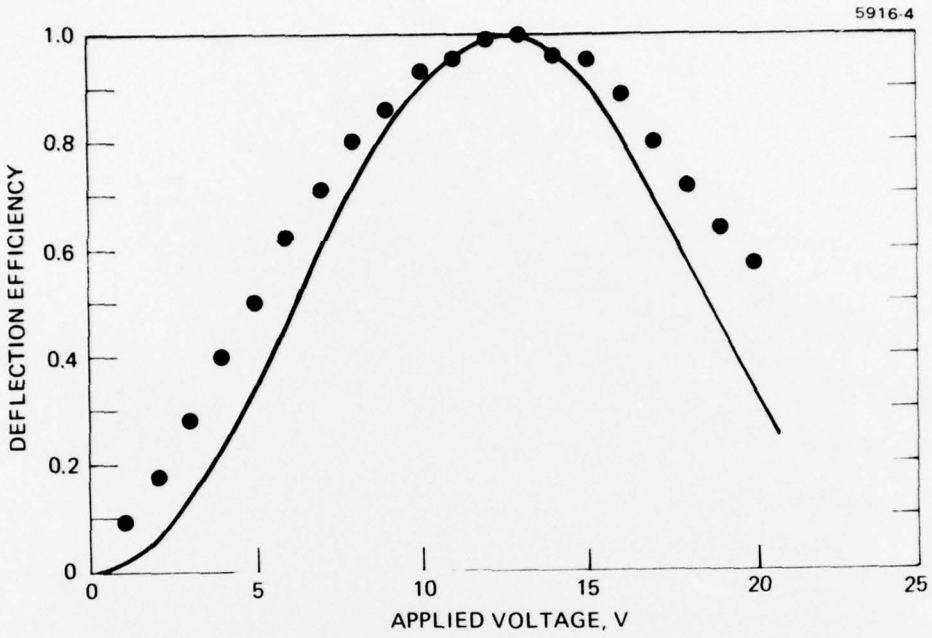

Fig. 10. Deflection efficiency vs. applied voltage for e-o Bragg switch (NB 23)

(b) Electrode Capacitance

The second important consideration of a switch device is the switching time, or the maximum operational bandwidth. For an electronic circuit of impedance R = 50 Ω, the bandwidth is mainly limited by capacitance. The capacitance of the interdigital electrodes is given by[4]

$$C = (\varepsilon_o + \sqrt{\varepsilon_{22}\varepsilon_{33}}) \frac{K(k)}{K'(k)} NL$$

where K(k) and K'(k) are the complete elliptic integral of the first kind with moduli k and k' respectively, N is the number of periods, ε_{22} and ε_{33} are the dielectric permittivity of the waveguide in the y and z directions. For the electrode structure used in this experiment, the numbers are

$$k' = k = \sin \frac{\pi}{4}$$

$$N = 10$$

$$L = 0.5 \text{ mm}$$

$$\varepsilon_{22} = 84\ \varepsilon_o$$

$$\varepsilon_{33} = 30\ \varepsilon_o$$

The capacitance of the electrode is then about 2.2 pF. This implies that maximum operational frequency could be as high as 3 GHz for a resistive load of R = 50 Ω.

(c) Drive Power

The drive power required to operate the Bragg switch may be expressed as

$$P_{dr} = \frac{V_m^2}{2R}$$

where V_m is the peak voltage for maximum diffraction into the first Bragg order and R is the resistive impedance in shunt with the capacitive grating electrodes. One chooses R to provide the desired RC-limited operating bandwidth $B = 1/\pi\ R\ C$. Thus

$$P_{dr} = \frac{\pi}{2} BC\ V_m^2$$

The figure of merit of this switch as described by power per megahertz of bandwidth becomes

$$\frac{P_{dr}}{B} = \frac{\pi}{2} C\ V_m^2 = 0.16 \text{ mW/MHz (sample NB 23)}$$

(d) Electro-optic Efficiency

A desirable feature for the optical waveguide switch is a high electro-optic efficiency. This means achieving a strong electrical field of the fundamental spatial harmonic in the region of greatest optical power density. The higher the overlap integral of electrical and optical fields over the depth direction, the smaller the electrical voltage required to achieve the maximum switching efficiency. In a switch device where electrical field is uniformly distributed over the whole interaction region, the maximum Bragg deflection occurs when the change of optical path $L\Delta n_i$ induced by the applied signal field equals one-half wavelength

$$L\Delta n_i = \lambda_o/2 \tag{1}$$

In $LiNbO_3$, the preferred crystallographic orientation calls for propagation along x or y with polarization and applied electric signal field along z. For this orientation

$$|\Delta n_i| = \frac{1}{2} n_e^3 r_{33} E_m \tag{2}$$

where n_e is the extraordinary refractive index, r_{33} is the appropriate electro-optic coefficient, and E_m is the peak signal field. For $n_e = 2.20$ and $r_{33} = 3.0 \times 10^{-9}$ cm/V, eqs. (1) and (2) give a half-wave field-length product

$$E_m \cdot L = \frac{\lambda_o}{n_e^3 r_{33}} = 1980 \text{ V.} \tag{3}$$

For the electrode dimensions used, L = 0.5 mm, s = 1 μm, the voltage required for maximum deflection is

$$V_m = 4 \text{ volts.} \tag{4}$$

In the configuration of waveguide switch, Bragg grating is formed by the fringe field of surface interdigital electrode. The cross-sectional view of electrode array and fringe field are depicted in Fig. 11. The electrical field in the z-direction in $LiNbO_3$ waveguide is given by[4]

$$E_z = \sum_{n=0}^{\infty} A_{2n+1} \cos\left[(2n+1)\frac{2\pi}{\Lambda} z\right] \exp\left[\frac{\varepsilon_{33}}{\varepsilon_{22}}(2n+1)\frac{2\pi}{\Lambda} y\right] \tag{5}$$

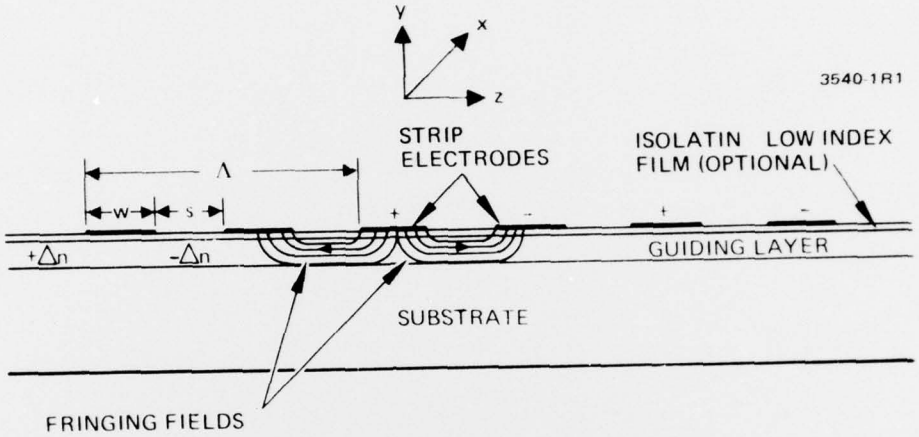

Fig. 11. Cross-sectional view of electrode array

The expansion coefficients A_{2n+1} are Legendre functions of the first kind.

$$A_{2n+1} = \frac{2\pi V}{\Lambda} \frac{P_n(2k^2-1)}{K'(k)} \tag{6}$$

where V is the voltage applied to electrodes, K'(k) is the complete elliptic integral of the first kind to the complementary modulus $k' = \sqrt{1-k^2}$

$$k = \cos\left[\frac{\pi}{2}\left(1 - \frac{2\omega}{\Lambda}\right)\right] \tag{7}$$

Since we are only interested in the fundamental Fourier component which satisfies Bragg deflection condition. In explicit form the fundamental component of E_z is given by

$$E_z = \frac{2\pi V}{\Lambda} \frac{1}{K'(k)} \cos\left[\frac{2\pi}{\Lambda} z\right] \exp\left[\frac{2\pi}{\Lambda} y\right] \tag{8}$$

The electrical field decays exponentially in the waveguide depth direction with 1/e point at $\Lambda/2\pi$ below surface.

On the other hand, the lowest order mode in a planar waveguide with a typical Gaussian index profile has its peak optical intensity at a depth of about 0.25 b below the surface, where b is the 1/e waveguide depth. We estimate the diffusion depth of NB 21 and NB 23 is about 2 μm, from which the overlap integral is calculated to be ∿0.3. Consequently, the peak deflection voltage for waveguide switch should occur at 4/0.3 = 13.3 volts which is in good agreement with the experimental value of 12.5 volts.

IV. Summary

This report, together with three previous quarterly reports, presents the design, development, fabrication and evaluation of an optical switch based on the deflection of two dimensionally confined beams by electro-optically controlled phase grating. The waveguide medium is Ti-diffused $LiNbO_3$. An interdigital electrode is placed on the overlapped region of two crossed channel waveguides. When a voltage is applied to the electrode, a Bragg phase grating is formed so that the optical beam in one channel waveguide is deflected into the opposite one and vice versa. In order to

interface the switching device to single mode optical fibers, narrow (4 μm wide) single mode channel waveguides are employed at the input and output ports. These waveguides are expanded adiabatically through slowly tapered sections into wide multimode channel waveguides (30 μm) that intersect in the grating interaction region.

The major effort during the initial period of this program was concentrated on two subjects, the fabrication of low loss single mode channel waveguides and the design of taper structures. An optimum diffusion schedule was developed so that high quality diffused waveguides could be fabricated routinely. Diffusions were normally carried out at temperature ranges from 850°C to 950°C in a flowing oxygen atmosphere. The diffusion time varied from 5 to 16 hours. Before diffusion, Ti-metal had been oxidized to TiO_2 at a relatively lower temperature (for instance, 600°C). The waveguide loss of 4 μm single mode channel waveguide was estimated to be about 1 dB/cm. For the waveguides thus formed there was no enhanced lateral diffusion along the crystal C-axis.

The design of expansion and contraction tapers is the crucial part of this program. If the taper is sufficiently gentle, the lowest order mode will be transmitted adiabatically, continuously readjusting to the slow variation of the guide width with virtually no reflection or coupling to higher order modes. In reality, one has to sacrifice the perfect adiabatic coupling in order to use a taper of reasonable length. As a first cut at the problem. linear tapers of taper lengths of 300, 600, 900 and 1200 μm were designed to expand channel guides from a 4 μm single mode channel to a 70 μm multimode channel. However, the measurement of coupling efficiency for TE and TM polarizations indicated that linear tapers were not efficient to preserve the mode structure even when the taper length was 1200 μm, 4000 times the He-Ne laser wavelength in the waveguide. A modification of initial switch design was incorporated into the program.

In order to achieve the goal of 90% single mode transmission efficiency, the width of expanded channel section was reduced from 70 μm to 30 μm and a taper formed out of three linear segments was

adopted. The channel waveguide width is expanded from 4 μm to 10 μm by the first linear taper of length 200 μm, from 10 μm to 20 μm by the second linear taper of length 500 μm, and from 20 μm to 30 μm by the third linear taper of length 800 μm. The full angles of these tapers are 1.72°, 1.15°, and 0.72°, respectively. The total length of this coupling horn structure is 1.5 mm. The experimental result indicated that a single mode coupling efficiency of 90% per taper for TM polarization had been achieved.

The second experimental phase involved the development of Bragg grating and integration with crossed channel waveguides. The grating is an interdigital electrode of spacing 4 μm and length 0.5 mm. Subsequent to the formation of the electrode pattern on the photoresist, the sample was coated with 1500 Å aluminum. Finally, Al metal electrode was formed by removing the photoresist and unwanted aluminum coated on the photoresist. The evaluation of the Bragg switch was carried out using two coupling prisms. Test light (He-Ne laser) was coupled into one channel guide at the input port. The power coming out of the channel guides at the output port was monitored as the voltage applied to the electrode varied. For sample NB 23, maximum switching efficiency (20%) occurred at voltages as low as 12.5 volts. Although the switching efficiency was lower than what we expected, we believed all the lowest order mode was deflected at interaction region as evidenced by the fact the switching efficiency obeyed the $\sin^2$ BV voltage dependence function and reached the maximum value at 12.5 volts. Most of the power remained in the undeflected channel guides were Li out-diffused modes generated at taper sections as well as Bragg coating region. We have developed a technique (under separate IRD funding) to eliminate Li out-diffusion waveguide by annealing the samples in $LiNbO_3$ powder. The interaction between metal electrode and optical beam can be avoided with a thin buffer layer (for instance, 2000 Å SiO_2) evaporated on the waveguide. With these improvements incorporated into the device, switching efficiency greater than 80% can be expected.

One of the most important measures of merit of optical switch is the drive power per bandwidth, which can be given by $\frac{\pi}{2} C V_m^2$, where C is the electrode capacitance and V_m is the applied voltage for maximum switching efficiency. For the switch we fabricated, V_m = 12.5 volts and C = 2.2 pF, the drive power per bandwidth is 0.16 mW/MHz. If the device is operated at bandwidth of 3 GHz, the drive power requires is about 5 W.

REFERENCES

1. G. L. Tangonan, "Thin Film Optical Switch," Quarterly Technical Report 1, Contract N00173-76-C-0113, May 1976.

2. B. Chen and G. L. Tangonan, "Thin Film Optical Switch," Mid-term Report, Contract N00173-76-C-0113, September 1976.

3. B. Chen and G. L. Tangonan, "Thin Film Optical Switch," Quarterly Technical Report 3, Contract N00173-76-C-0113, November 1976.

4. H. Engan, IEEE Trans. Electron. Devices ED-6, 1014 (1969).